npg

ORIGINAL ARTICLE

Liquid deposition photolithography for submicrometer resolution three-dimensional index structuring with large throughput

Adam C Urness, Eric D Moore, Keith K Kamysiak, Michael C Cole and Robert R McLeod

Photonic devices increasingly require three-dimensional control of refractive index, but existing fabrication methods such as femtosecond micromachining, multilayer lithography and bulk diffusion can only address a select scale range, are often limited in complexity or thickness and have low throughput. We introduce a new fabrication method and polymeric material that can efficiently create mm^3 optical devices with programmable, gradient index of refraction with arbitrary feature size. Index contrast of 0.1 is demonstrated, which is 100 times larger than femtosecond micromachining, and 20 times larger than commercial holographic photopolymers. This is achieved by repetitive microfluidic layering of a self-developing photopolymer structured by projection lithography. The process has the unusual property that total fabrication time for a fixed thickness decreases with the number of layers, enabling fabrication 10^5 faster than femtosecond micromachining. We demonstrate the process by sequentially writing 100 layers to fabricate a mm thick waveguide array.

INTRODUCTION

Three dimensional index structuring is currently accomplished by multiphoton direct-write lithography[1] at a scanning point, multilayer projection lithography[2] of sequential two-dimensional (2D) planes or volume holography[3] of entire three-dimensional (3D) volumes. While submicrometer resolution is possible in all cases, throughput dramatically increases with dimensionality of the exposure but at the cost of flexibility in the type of structure that can be fabricated. In the case of direct-write lithography, multiphoton absorption is utilized to restrict out-of-focus response. Unfortunately, multiphoton absorption requires femtosecond pulse length for efficient excitation. Glass is the most used base material and has high environmental stability, but requires irradiances of $10^{17}\,\mathrm{W\,m^{-2}}$ or larger[1] and device thickness is restricted to the working distance of an oil-immersion objective. Most applications are sparse waveguide[4–7] devices, though dense 3D index patterns such as volume computer generated holograms[8] have been generated, but only contain 64^3 features. To increase throughput and eliminate depth restrictions, liquid polymers[9] containing photo-initiators with large two-photon cross-sections and polymerization chain reactions to increase sensitivity are used. Sparse waveguide[10,11] devices have been fabricated and scanning point exposures have created dense 3D structures including invisibility cloaks[12] and templates for a gold polarizer.[13] However, even with the increased throughput of polymers, the fabrication rate for the polymer structure of the

invisibility cloak is 13 years mm^{-3} (see Supplementary Information), because the necessary power density still requires rastering through a large number of very small voxels, limiting devices to sparse, typically binary structures with small voxel count.

To increase throughput over a scanning single point, a single 2D exposure writes a multitude of features simultaneously. Two-photon absorption cannot be used, because response greatly reduces over a large transverse area, therefore one photon absorption must be used. However, one-photon absorption does not restrict out-of-focus response, so 2D exposures are typically done into a thin layer. Ultraviolet (UV) optical projection lithography is the most common and has better resolution and many orders of magnitude larger throughput than scanning point, two photon lithography. Repetitive projection lithography and planarization enables both large area and arbitrary 3D structuring, demonstrated by the fabrication of a 3D optical metamaterial.[7] However, each high-throughput 2D layer is followed by hours of processing in a series of tools, currently limiting demonstrations to four layers.

The depth limit of sequential 2D processing can be avoided by 3D holographic exposure. One photon diffusion driven photopolymers[14] enable self-developing 3D patterning of up to cm thick solid volumes. These materials contain two monomers,[15] in which the first monomer thermally gels providing a physical scaffold for index structures. Incident light polymerizes the second monomer, locally depleting

2

monomer in the exposed region. This causes diffusional mass transport of unreacted monomer into the exposed region, resulting in an increased material density and index of refraction, without solvents or thermal processing. A postexposure optical flood cure is then done to bleach remaining initiator and cross-link all remaining monomer. The low required dose ($\sim$100 mJ cm^{-2}) and wavelength sensitivity (UV to near infrared) of these materials have lead to applications in optical data storage[16] with 1.6 TB capacity and 960 Mbit s^{-1} data rates, photonic devices such as waveguides,[17] holographic filters[18] and GRIN lense.[19] However, one-photon absorption in solid, thick materials does not yield complete control of the 3D index distribution due to diffraction. Additionally, the required diffusion time for development increases quadratically with scale, limiting maximum feature size to hundreds of micrometers.

Here we show a new fabrication process, liquid deposition photolithography (LDP), and a one-photon, initially liquid photopolymer to fabricate submicrometer resolution 3D index structures. The fabricated 3D index structures have an index contrast up to 0.1, 100 times larger than femtosecond micromachining,[1] allowing greater flexibility in device fabrication. High throughput is enabled by using an initially liquid photopolymer, which allows microfluidic manipulation and rapid monomer diffusion. The 3D volume is created through repetitive layering, where each layer is structured by projection lithography. Every processing step is performed on a single instrument, vastly reducing fabrication time compared to multilayered semiconductor lithography. With this process and material we demonstrate 3D index structures throughout hundreds of layers with a fabrication rate of 1.2 h mm^{-3}.

MATERIALS AND METHODS

Materials

The photopolymer used in this work was made using solutions of 0.7 wt-% Irgacure 651 (Sigma Aldrich), 94.3 wt-% poly(ethylene glycol)-di(urethane methacrylate) (synthesized) and 5 wt-% tribromo phenyl acrylate (Polymer Sciences). The poly(ethylene glycol)-di(urethane methacrylate) was synthesized by mixing 92.7 wt-% glycerol propoxylate mw $\sim$4300 (Sigma Aldrich), 7.2 wt-% isocyanethyl methacrylate (Sigma Aldrich) and 0.1 wt-% dibutyltin dilaurate (Sigma Aldrich) over 40℃ heat for 10 h. All components were used as received without additional purification.

Chamber window fabrication

Chamber windows were fabricated by adhering a flat, 125-μm layer of polydimethylsiloxane (PDMS, Sylgard 184; Dow Corning) onto microscope cover slips (Ted Pella, 22×50 mm). To create a flat PDMS surface, the PDMS and cover slips were cast against BK7 float glass and peeled off after the PDMS thermally cured. To set the thickness of the PDMS layer, 125-μm spacers were placed between the cover glass and BK7 float glass. To promote PDMS adhesion to the cover glass and prevent PDMS adhesion to the BK7 float glass, they were treated with Dow Corning P5200 adhesion promoter and (tridecafluoro-1,1,2,2-tetrahydroctyl) trimethoxysilane, respectively. The samples were put in an oven at 100℃ for 2 h to thermally cure the PDMS.

RESULTS AND DISCUSSION

The process steps of LDP are shown in Figure 1. Figure 2 illustrates the process of high-resolution 3D index structuring *via* a 1-μm-thick
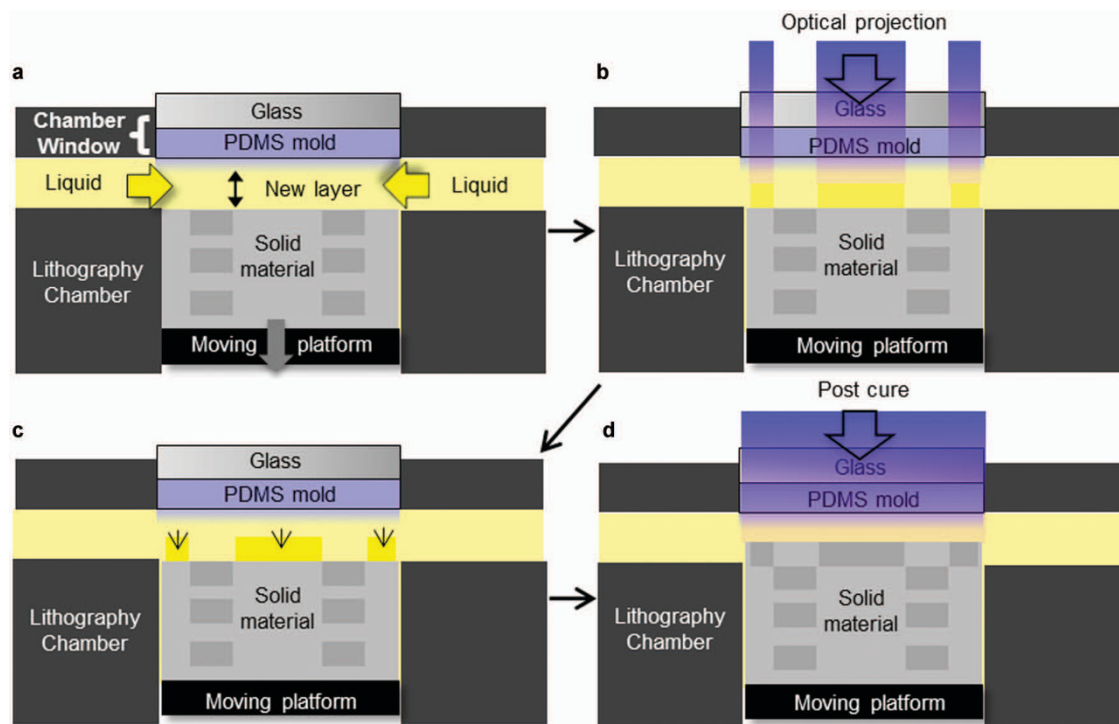

Figure 1 Steps of LDP process. (**a**) UV-sensitive liquid monomer is drawn through a microfluidic channel created as the platform is lowered, producing a new layer. (**b**) The new liquid layer is patterned by 2D projection lithography, using 365 nm light, polymerizing the liquid monomer into a solidified gel of the 2D pattern. Polymerization is suppressed just below the window *via* inhibitor diffusion from the PDMS mold. (**c**) Unreacted monomer diffuses from this adjacent layer of liquid monomer into the solid to replace that consumed by polymerization. This diffusion increases the material density and index of refraction in the exposed region. (**d**) The entire layer is optically flood-cured, using 365 nm light, to a solid, cross-linked, photo-insensitive polymer. Steps (**a**)–(**d**) are rapidly repeated to fabricate complex 3D index structures.
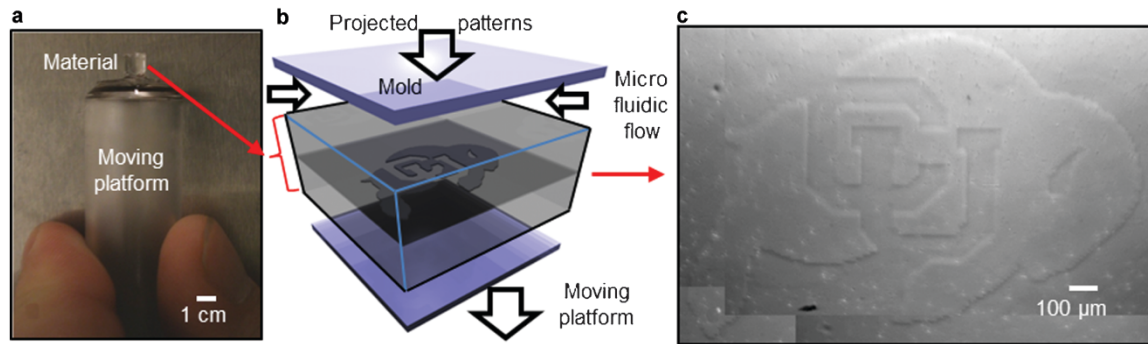
Figure 2 Example fabrication using the LDP instrument. (**a**) Photo of a fabricated part deposited on LDP platform. (**b**) Deposition chamber and three-layer part layout. The three layers consist of a thick, non-patterned layer, a 1-μm-thick layer patterned by 2D projection lithography and a final thick, non-patterned layer. (**c**) DIC phase micrograph of the part shown in (**b**).

index pattern sandwiched between two unstructured layers each 2 mm thick. In addition to full 3D control of index, processing time in LDP is reduced compared to multilayered planar lithography, because the material is self-developing, enabling the entire process to be completed on a single instrument. This eliminates the additional instruments in multilayered planar lithography that are required for layer planarization and chemical and thermal processing. Similar to planar lithography, transverse resolution is a function of the projection optics, material response and layer thickness, while axial resolution is determined by layer thickness. In LDP the layer is not spin coated but, instead, fluid is deposited by the motion of a stage with nanometer resolution and planarized by the chamber window.

The chamber window, a flat, 125-μm-thick PDMS layer that is adhered to cover glass, was originally developed to allow optical pattern access and prevent polymer adhesion to the window for efficient fabrication of micrometer-sized particles.[20] We have extended the use to passively planarize new layers as a mold and maintain a monomer-rich liquid layer next to the exposed part. The chamber window performs these functions by providing a constant flux of oxygen at the liquid monomer boundary *via* diffusion from the PDMS layer. Oxygen is a strong radical inhibitor,[21] so polymerization is prevented in the thin liquid monomer layer directly adjacent to the chamber window. Oxygen is used as the inhibitor, because it is naturally present *via*

atmospheric diffusion, is a well-characterized inhibitor of radical polymerization and diffuses rapidly due to its small size. Details of the inhibition process are revealed in a reaction/diffusion simulation shown in Figure 3a. The simulation shows that the oxygen is consumed by photogenerated radicals at all depths, except near the window where it is continually replenished *via* diffusion from the PDMS. This inhibits conversion in a 1-μm layer, preventing adhesion of polymer to the window and providing a high-concentration monomer source for subsequent diffusional mass transport into the exposed layer.

Rapid fabrication of thick, high axial resolution devices is made possible by the short diffusion path from the liquid layer. The time to fabricate a single layer consists of the mask translation and settle time, exposure duration and monomer diffusion time. The diffusion time scales as the layer thickness squared while the exposure time is not dependent on layer thickness. Therefore, for a fixed part thickness, total diffusion time for all layers decreases linearly with layer thickness, as shown in Figure 3b. The relationship between axial resolution and fabrication time is therefore unusual, in that higher resolution causes faster write times. This relation breaks down for sufficiently thin layers where exposure duration and mask translation and settle time dominate.

During the process of monomer diffusion, a solid matrix material is required to provide a physical scaffold. In one-component photopolymers, this scaffold is formed by incomplete polymerization of a
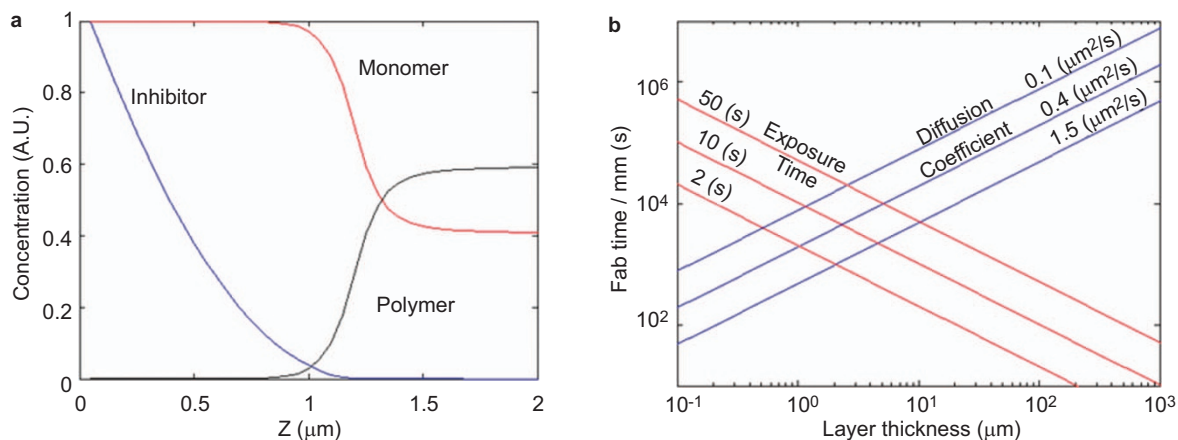

Figure 3 Reaction/diffusion simulations of LDP. (**a**) Concentration of inhibitor, monomer and polymer immediately after completion of exposure. (**b**) Total time required to complete exposure and diffusion of a 1-μm-thick part as a function of the individual layer thickness for various per layer exposure times and diffusion coefficients for materials similar to the material used for the experiments shown here. There is an optimal layer thickness, depending on both the exposure time and monomer diffusion constant, which is on the order of 1 μm.

single monomer. Photopolymerization and diffusion of the remaining monomer creates the index pattern. As shown in Ref. 15, this results in low index contrast. Two-component photopolymers use a low-index, thermal-set matrix and a high-index diffusing monomer, resulting in high index contrast, but the thermal-set matrix cannot be sequentially layered. As shown in Figure 4, we use a two-component mixture in which both the matrix and high-index diffusing monomer are liquid photopolymers. Rapid polymerization of the methacrylate matrix is followed by diffusion and then polymerization of the slower acrylate monomer. This formulation can be injected and photocured into thin layers like a one-component photopolymer but achieves the high-index contrast typical of two-component photopolymers. As shown in Figure 5a, we demonstrate the index contrast to be 0.1, 20 times larger than commercial grade holographic photopolymers.[22] The large index contrast is a result of both the process, which uses photopolymers in the liquid state enabling full dynamic range of polymerization and high monomer mobility and the material design. To demonstrate the efficacy of this material design, a material without high-index monomer develops very low index contrast as shown in Figure 4e, but a material with high-index monomer under the same exposure conditions exhibits much stronger contrast, as shown in Figure 4f.

With this process and material we demonstrate fabricated volumes of 100 layers containing 3D index structures, with index contrasts 100 times larger and fabrication rates 10^5 times faster than femtosecond micromachining. Figure 5a shows a phase micrograph of a 1-μm-thick University of Colorado (CU) buffalo pattern, followed by a 1-μm-thick

CU seal pattern, demonstrating the ability to stack multiple, different layers. Figure 5b shows a 1-μm pitch hologram, corresponding to 500 nm line widths, written using two beam interference, demonstrating both analog response and submicrometer transverse resolution. Furthermore, holographic media testing[22] reveals an achievable material transverse resolution of 143 nm, documented in the Supplementary Information. By stacking multiple, thin layers this process can fabricate 3D diffractive structures which cannot be made with traditional multiple beam interference. Figures 5c demonstrates the flexibility of LDP *via* a photonic crystal waveguide structure. To demonstrate LDPs ability to fabricate a unique photonic device, 100 layers were sequentially patterned and stacked to create a millimeter-thick rectangular waveguide array shown in Figure 5d–f. The index contrast of the waveguide array, measured by a scanning optical microscope,[23] was measured to be 0.1, as shown in Figure 5f.

CONCLUSIONS

In summary, the LDP process together with a novel two-component liquid photopolymer enable efficient production of gradient index structures with arbitrary index feature size and shape not limited by out of focus exposure. The gradient index structures have an index contrast of 0.1, allowing greater flexibility and design of 3D refractive index devices. By using a liquid, self-developing photopolymer that is manipulated through microfluidics and a chamber window that automatically planarizes each new layer, processing of multiple layers is done on a single instrument, minimizing fabrication time.
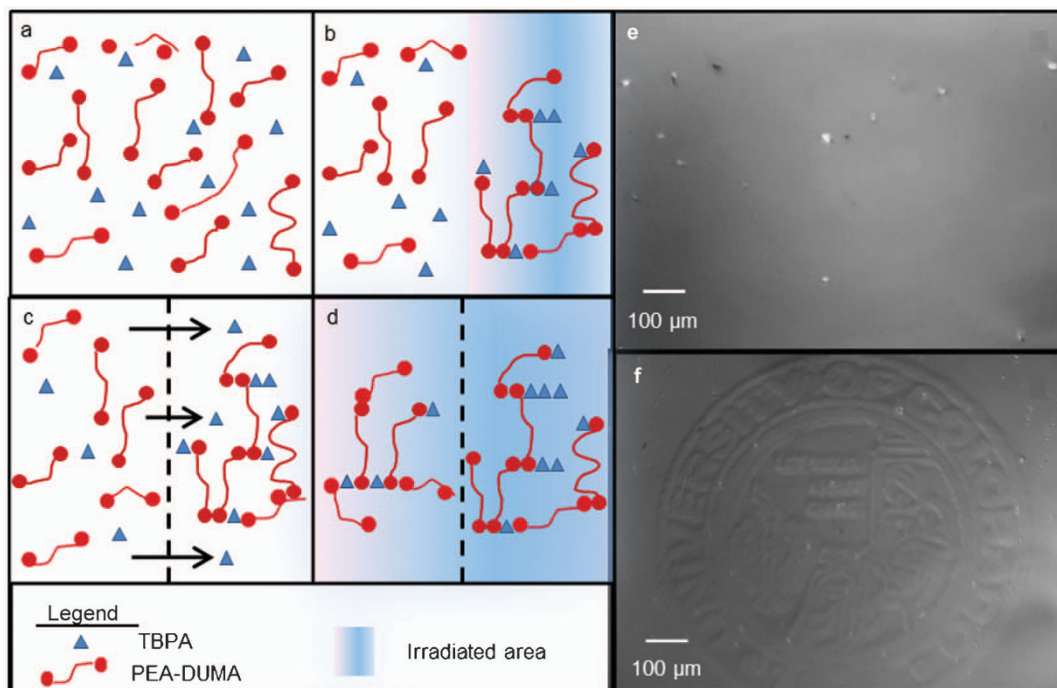

Figure 4 Material function. To maximize index contrast the material formulation contains two photopolymerizable monomers with different refractive indices and molecular weights. The low index, high molecular weight monomer, PEA-DUMA, is represented by two red circles connected by a line indicating its two functional groups. The high index, low molecular weight TBPA is represented by a single blue triangle indicating its single functional group. (**a**) The mixture of photo-initiator and monomers are injected into the exposure region in the form of a thin liquid layer. (**b**) A portion of the area is exposed which locally consumes both monomers creating a low-index solid. (**c**) Due to its smaller molecular weight, TBPA preferentially diffuses in to replace that consumed by polymerization, increasing the index of the exposed region. Note that in the LDP system, the majority of this diffusion is out of the inhibited layer through the thin depth of the part, not transversely across the large part width. (**d**) After the mass transport of TBPA has concluded, the entire layer is exposed, polymerizing the remaining monomer to create a solid, cross-linked, insensitive polymer with approximately uniform PEA-DUMA and photo-patterned TBPA. (**e**) In this control experiment, the TBPA was not present. The phase micrograph of the 3-μm-thick structure shows no measurable index change. (**f**) Phase micrograph of a 3-μm-thick index structure with the same exposure conditions as (**e**), but containing TBPA.
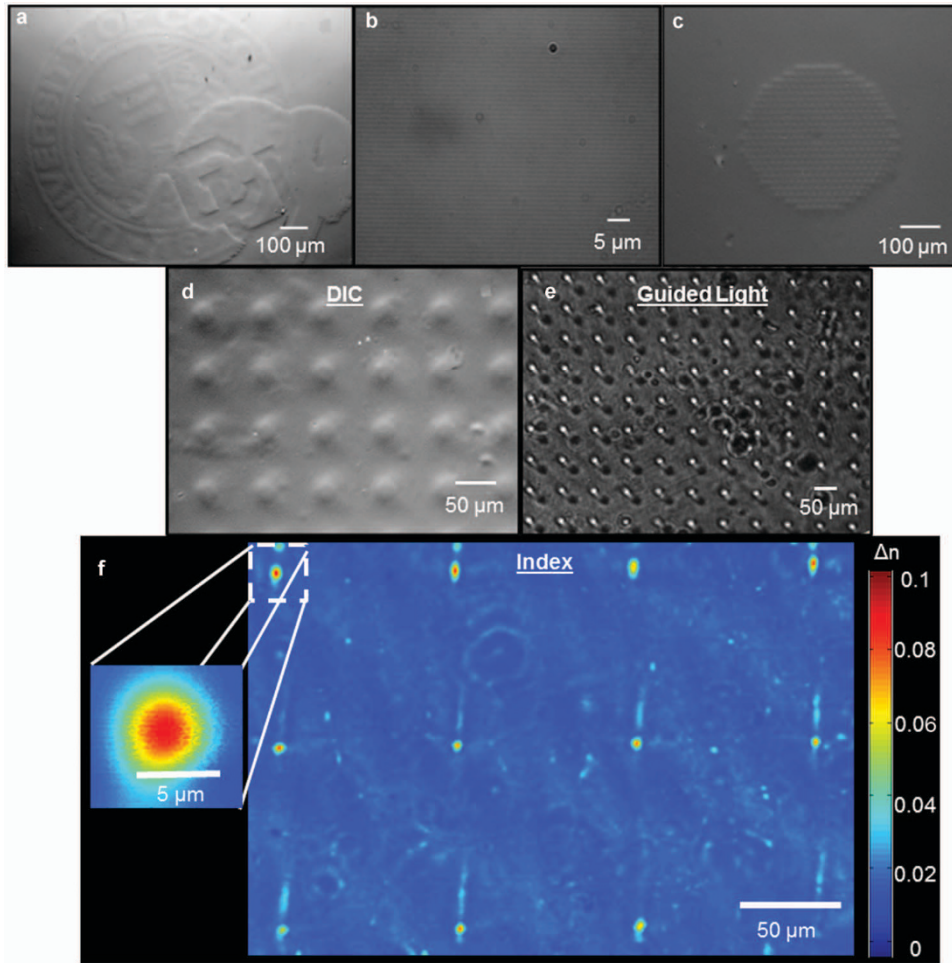
Figure 5 Index structures written with LDP. (**a**) Two sequentially written 3 μm layers of the buffalo, written first, and the CU seal, written second, demonstrating multiple layer fabrication. (**b**) 1 μm pitch hologram demonstrating submicrometer resolution transversely. (**c**) Phase micrograph of a photonic crystal fiber written in a 3-μm layer. (**d**) Phase micrograph of a 60-μm pitch rectangular waveguide array pattern written in a single 10-μm layer. (**e**) Image of the end facet of 80 μm pitch rectangular waveguide array, fabricated by sequentially writing 100, 10-μm-thick layers, where the front facet was illuminated with a plane wave at 633 nm. (**f**) Refractive index map of the end facet of the rectangular waveguide array shown in (**d**) and (**e**).

Total fabrication time is independent of transverse feature scale and density but decreases with increased axial resolution, enabling rapid fabrication of high resolution devices. This technique could be used to fabricate arbitrary 3D refractive index devices such as photonic crystal waveguides,[24] diffractive elements such as volume computer generated hologram's and 3D integrated photonic devices.

1 Gattas RR, Mazur E. Femtosecond laser micromachining in transparent materials. *Nat Photon* 2008; **2**: 219–225.

2 Liu N, Guo H, Fu L, Kaiser S, Schweizer H *et al*. Three-dimensional photonic metamaterials at optical frequencies. *Nat Mater* 2008; **7**: 31–37.

3 Colburn WS, Haines KA. Volume hologram formation in photopolymer materials. *Appl Opt* 1971; **10**: 1636–1641.

4 Davis KM, Miura K, Sugimoto N, Hirao K. Writing waveguides in glass with a femtosecondlaser. *Opt Lett* 1996; **21**: 1729–1731.

5 Sikorski Y, Said AA, Bado P, Maynard R, Florea C *et al*. Optical waveguide amplifier in Nd-doped glass written with near-IR femtosecond laser pulses. *Electr Lett* 2000; **36**: 226–227.

6 Streltsov AM, Borrelli NF. Fabrication and analysis of a directional coupler written in glass by nanojoule femtosecond laser pulses. *Opt Lett* 2001; **26**: 42–43.

7 Kowalevicz AM, Sharma V, Ippen EP, Fujimoto JG. Three-dimensional photonic devices fabricated in glass by use of a femtosecond laser oscillator. *Opt Lett* 2005; **30**: 1060–1062.

8 Gerke TD, Piestun R. Aperiodic volume optics. *Nat Photon* 2010; **4**: 188–193.

9 Cumpston BH, Ananthavel SP, Barlow S, Dyer DL, Ehrlich JE *et al*. Two-photon polymerization initiators for three-dimensional optical data storage and microfabrication. *Nature* 1999; **398**: 51–54.

10 Zoubir A, Lopez C, Richardson M, Richardson K. Femtosecond laser fabrication of tubular waveguides in poly(methyl methacrylate). *Opt Lett* 2000; **29**: 1840–1842.

11 Sowa S, Watanabe W, Tamaki T, Nishii J, Itoh K. Symmetric waveguides in poly(methyl methacrylate) fabricated by femtosecond laser pulses. *Opt Express* 2006; **14**: 291–297.

12 Ergin T, Stenger N, Brenner P, Pendry JB, Wegener M. Three-dimensional invisibility cloak at optical wavelengths. *Science* 2010; **16**: 337–339.

13 Gansel JK, Thiel M, Rill MS, Decker M, Bade K *et al*. Gold Helix photonic metamaterial as broadband circular polarizer. *Science* 2009; **325**: 1513–1515.

14 Zhao G, Mouroulis P. Diffusion model of hologram formation in dry photopolymer materials. *J Modern Opt* 1994; **41**: 1929–1939.

15 Dhar L, Hale A, Katz HE, Schilling ML, Schnoes MG *et al*. Recording media that exhibit high dynamic range for digital holographic data storage. *Opt Lett* 1999; **24**: 487–489.

16 Dhar L, Curtis K, Facke T. Holographic data storage: coming of age. *Nat Photon* 2008; **2**: 403–405.

17 Sullivan AC, Grabowski MW, McLeod RR. Three-dimensional direct-write lithography into photopolymer. *Appl Opt* 2007; **46**: 295–301.

18 Sato A, Scepanovic M, Kostu RK. Holographic edge-illuminated polymer Bragg gratings for dense wavelength division optical filters at 1550 nm. *Appl Opt* 2003; **42**: 778–784.

19 Ye C, McLeod RR. GRIN lens and lens array fabrication with diffusion-driven photopolymer. *Opt Lett* 2008; **33**: 2575–2577.

20 Dendurkuri D, Pregibon DC, Collins J, Hatton TA, Doyle PS. Continuous flow lithography for high-throughput microparticle synthesis. *Nat Mater* 2006; **5**: 365–369.

21 Decker C, Jenkins AD. Kinetic approach of O_2 inhibition in ultraviolet- and laser-induced polymerizations. *Macromolecules* 1985; **18**: 1241–1244.

22 Curtis K, Dhar L, Hill A, Wilson W, Ayres M. Holographic Data Storage: From Theory to Practical Systems. Wiley; 2010.

23 Wilson T, Gannaway JN, Sheppard CJR. Optical fibre profiling using a scanning optical microscope. *Opt Quant Electr* 1980; **12**: 341–345.

24 Riishede J, Lægsgaard J, Broeng J, Bjarklev A. All-silica photonic bandgap fibre with zero dispersion and a large mode area at 730 nm. *J Opt A Pure Appl Opt* 2004; **6**: 667–670.